Proceedings of the 2000 IEEE
International Conference on Robotics & Automation
San Francisco, CA • April 2000

Vision-Based Dynamic Estimation and Set-Point Stabilization of Nonholonomic Vehicles

F. Conticelli
Scuola Superiore Sant'Anna
Via Carducci 40, I-56127
Pisa, Italy

D. Prattichizzo
Dept. Information Engineering
University of Siena, Italy

F. Guidi A. Bicchi
Dept. Electrical Systems and Automation
University of Pisa, Italy

Abstract

In this paper, a nonholonolonomic vehicle is stabilized to a desired pose through a visual servoing technique. The vision-based regulation of the nonholonomic vehicle, we propose, is built through a discontinuous change of coordinates and Lyapunov-based design, which ensure asymptotic stability of the closed-loop visual system. A dynamic estimation procedure, based on the optical flow equations, is also presented to deal with uncertainties in the observed environment. Simulations results on an autonomous mobile robot are reported, that show the practicality of the proposed approach.

1 Introduction

Path planning and control of nonholonomic robots have been widely investigated in the literature [5, 2, 11, 12, 10]. Wheeled mobile robots lead to intrinsic nonlinear control problems, since linearization around a fixed equilibrium is uncontrollable, and it is also not possible to stabilize the nonhonolonomic system to a given set-point by a continuous and time-invariant feedback control [4]. In the literature two different approaches have been used to solve the point stabilization problem [10, 1], one uses a time-varying state feedback while the other avoids the problem pointed out in [4] by means of discontinuous feedback. The control law considered in this paper belongs to the second family of stabilizing controllers. The nonlinear control problem results to be more involved because of the visual feedback. Visual servoing have been recently applied to mobile robotics [7, 13, 6]. It essentially consists of defining the control goals and designing the feedback law directly in the image domain. Designing the feedback at the sensor level increases system performances especially when uncertainties and disturbances affect the robot model and the camera calibration, see [8] and therein references. In [8] the authors also present a classification of visual servoing systems. The approach here is known as image-based visual servoing, the error between the robot pose with respect to a target object or a set of target features is computed directly in terms of image features, since any visual task is described in the image plane as a desired evolution of object appearance towards a goal one.

This paper deals with the problem of controlling the pose of a nonholonomic mobile robot with respect to a target object. The mobile robot is equipped with a camera grabbing the object cues whose image plane projections are stabilized to desired positions through the visual servoing procedure. The paper is organized as follows. Section 2 introduces the camera-object visual interaction model in terms of the planar optical flow equations. In Section 3, the control system is synthesized, after the reduction of the configuration space coordinates, and the introduction of a discontinuous diffeomorphism in the state space. In Section 4, the 3-D parameters characterizing the target object are estimated through a robot self-calibration procedure, while during the control task execution an on-line gradient-based update can be also performed. Section 5 reports simulation results carried out to validate the theoretical framework. Finally, in Section 6 the major contribution of the paper is summarized.

2 Visual Modeling

We consider a unicycle model of a robotic vehicle, with a reference frame $< c >= \{x_c, y_c, z_c\}$ fixed on it. Let the configuration of the unicycle be described by $\boldsymbol{q} = [X,\ Y,\ \theta]^{\mathrm{T}}$ (see fig. 1). The control input to the mobile robot is the steering velocity $\omega = \dot{\theta}$ and the translational velocity v along the z_c axis. Assume that a pinhole camera is fixed to the unicycle and that

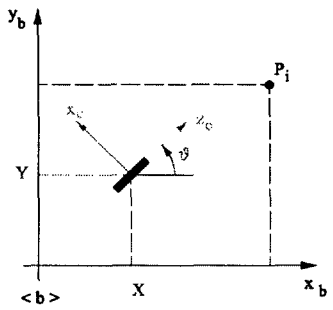

Figure 1: Notation for the unicycle with a fixed camera mounted on.

its camera frame is $< c >$, where z_c is the optical axis of the camera, and y_c is parallel to z_b. Consider a set of $n \geq 2$ fixed point features in the environment, whose coordinates in the moving frame $< c >$ are $\boldsymbol{P}_i = [X_i,\ Y_i,\ Z_i]^T$, and notice that, because the vehicle moves in a plane, $Y_i \stackrel{def}{=} h_i$ is costant. For the remaining coordinates of $\boldsymbol{P}_i$, one has

$$\begin{bmatrix} \dot{X}_i \\ \dot{Z}_i \end{bmatrix} = \begin{bmatrix} -Z_i\,\omega \\ -v + X_i\,\omega \end{bmatrix}. \tag{1}$$

Equation 1 is a nonlinear dynamic system, affine in the control inputs and without drift term. Under the assumption that the projective geometry of the camera is modeled by perspective projection, the point $\boldsymbol{P}_i = [X_i, h_i, Z_i]^T$, will project, if $Z_i \neq 0$, onto the image plane (x_c, y_c) as $x_i = \frac{f\,X_i}{Z_i}$, $y_i = \frac{f\,h_i}{Z_i}$, where f is the focal length of the camera lens. Assuming $h_i \neq 0$, the full perspective projection can be inverted as $X_i = \frac{h_i x_i}{y_i}$, $Z_i = \frac{f h_i}{y_i}$. By deriving camera projection equation, from (1), it ensues that the optical flow of $\boldsymbol{P}_i$ in the image plane is

$$\begin{bmatrix} \dot{x}_i \\ \dot{y}_i \end{bmatrix} = \begin{bmatrix} -\frac{x_i\,y_i}{f\,h_i} & \frac{f^2+x_i^2}{f} \\ -\frac{y_i^2}{f\,h_i} & \frac{x_i\,y_i}{f} \end{bmatrix} \begin{bmatrix} v \\ \omega \end{bmatrix}. \tag{2}$$

3 Set-point stabilization

Assume that features are sufficiently many and are distributed in space such that the collection of their coordinates in the image plane, $\mathbf{x} = [x_1, y_1, \ldots, x_n, y_n]$, uniquely determines the robot configuration. The differential kinematic model of the visual interaction of the robot with the environment is described by the $2n$ optical flow equations (2) of the image vector $\mathbf{x}$. This section deals with the problem of stabilizing the image vector $\mathbf{x}$ with respect to a constant reference vector $\mathbf{x}_{des}$, in the assumption (to be removed in the next section) that the constant heights of points $\boldsymbol{P}_i$ are known. Notice that, although $\mathbf{x}$ is a point in a $2n$ dimensional space, its evolution is constrained on a submanifold of dimension 3, which is locally diffeomorphic to the vehicle's configuration space $\mathbb{R}^2 \times S^1$. Therefore, in the absence of noise, stabilization of any three independent combinations of components of $\mathbf{x}$ would guarantee stabilization of the whole image, hence of the vehicle. However, image points will inevitably be affected by measurement errors; moreover, visual occlusions might exclude from view those features that have been chosen for visual servoing. In view of this considerations, and to introduce some robustness to measurement errors and occlusions, we introduce a 3-dimensional state vector $\boldsymbol{\xi}$ that incorporates information from all visual cues in the image.

Let the displacement between the actual and desired position of the i–th feature be $\delta_i = [X_i - X_{i,des}, Z_i - Z_{i,des}]^T$, and denote with ψ the angular displacement between the lines through the actual and the desired positions of the i–j pair of features. be represented as

$$\begin{bmatrix} X_j \\ Z_j \end{bmatrix} - \begin{bmatrix} X_i \\ Z_i \end{bmatrix} = R \left(\begin{bmatrix} X_{j,des} \\ Z_{j,des} \end{bmatrix} - \begin{bmatrix} X_{i,des} \\ Z_{i,des} \end{bmatrix} \right) \tag{3}$$

where

$$R = \begin{bmatrix} \cos\psi & \sin\psi \\ -\sin\psi & \cos\psi \end{bmatrix}. \tag{4}$$

Assuming a uniformly distributed normal noise on the measurement of $\mathbf{P}_i$, $i = 1, \ldots, n$, the best estimate of the linear displacement is the average value

$$\delta = \frac{\sum_{i=1}^n \delta_i}{n} = \begin{bmatrix} \frac{\sum_{i=1}^n X_i}{n} \\ \frac{\sum_{i=1}^n Z_i}{n} \end{bmatrix} - \begin{bmatrix} \frac{\sum_{i=1}^n X_{i,des}}{n} \\ \frac{\sum_{i=1}^n Z_{i,des}}{n} \end{bmatrix}.$$

The third component of vector ξ can be obtained as an estimate of ψ from all equations of the form (3) with $i < j$. Notice that obtaining an optimal estimate of ψ is more involved, due to constraints on the orthonormality of the rotation matrix appearing in (3): constrained optimization techniques should therefore be adopted, such as those reported in [9]. By using the full perspective transformation, the (unperturbed) dynamics of the reduced coordinate vector ξ can be written in terms of the parameters h_i, $i = 1, \ldots, n$ as

$$\begin{bmatrix} \dot{\xi}_1 \\ \dot{\xi}_2 \\ \dot{\xi}_3 \end{bmatrix} = \begin{bmatrix} -f\xi_2 u_2 \\ \frac{1}{f} u_1 + \frac{\xi_1}{f} u_2 \\ -u_2 \end{bmatrix}. \tag{5}$$

where control inputs are defined as $u_1 = v$ and $u_2 =$

$-\omega$. Consider the change of coordinates

$$\begin{bmatrix} r_1 \\ r_2 \\ r_3 \end{bmatrix} = \begin{bmatrix} \sin(\xi_3)\xi_1 + \cos(\xi_3)\xi_2 f \\ \cos(\xi_3)\xi_1 - \sin(\xi_3)\xi_2 f \\ -\xi_3 \end{bmatrix}, \quad (6)$$

which represents a global diffeomorphism since $f \neq 0$ and define the error vector z

$$\begin{cases} z_1 = r_1 - r_1^{(d)} \\ z_2 = r_2 - r_2^{(d)} \\ z_3 = r_3 \end{cases}, \quad (7)$$

whose dynamics can be written as

$$\begin{bmatrix} \dot{z}_1 \\ \dot{z}_2 \\ \dot{z}_3 \end{bmatrix} = \begin{bmatrix} \cos(z_3)u_1 \\ \sin(z_3)u_2 \\ u_2 \end{bmatrix}. \quad (8)$$

Hence, the dynamics of the optical flow (in the above assumptions) are equivalent, up to a coordinate change, to those of a unicycle [1]. To stabilize the nonlinear dynamics in eq. (8), the approach used in [1] might be applied by rewriting the system in polar coordinates, i.e.

$$\begin{cases} \rho = \sqrt{z_1^2 + z_2^2} \\ \alpha = -z_3 + \arctan 2\left(-\frac{z_2}{\sqrt{z_1^2+z_2^2}}, -\frac{z_1}{\sqrt{z_1^2+z_2^2}}\right) \\ \phi = \arctan 2\left(-\frac{z_2}{\sqrt{z_1^2+z_2^2}}, -\frac{z_1}{\sqrt{z_1^2+z_2^2}}\right) \end{cases}. \quad (9)$$

The corresponding dynamics results

$$\begin{bmatrix} \dot{\rho} \\ \dot{\alpha} \\ \dot{\phi} \end{bmatrix} = \begin{bmatrix} -\cos(\alpha)u_1 \\ -u_2 + \frac{\sin(\alpha)}{\rho}u_1 \\ \frac{\sin(\alpha)}{\rho}u_1 \end{bmatrix}, \quad (10)$$

which can be asymptotically stabilized by means of a Lyapunov-based design [1], leading to the following closed-loop control law

$$\begin{cases} u_1 = k_1 \cos(\alpha)\rho \\ u_2 = k_2\alpha + k_1 \frac{\cos(\alpha)\sin(\alpha)}{\alpha}(\alpha + k_3\,\phi) \end{cases}. \quad (11)$$

A simulative analysis of the closed loop system performance shows the presence of cusps in the state trajectory, corresponding to backward motions of the vehicle, that would lead to loose visibility of the image features. The occurrence of cusps are due to inversions of the sign of the control input u_1 and, in an application using visual servoing, makes the method of [1] inapplicable. In what follows, we present therefore a modified version of control law (11) with the aim of avoiding motion inversion during visual servoing. Consider the feedback control law

$$\begin{cases} u_1 = k_1\bar{\rho} \\ u_2 = k_2\bar{\alpha} + k_1\frac{\sin(\bar{\alpha})}{\bar{\alpha}}(\bar{\alpha} + k_3\,\bar{\phi}) \end{cases}, \quad (12)$$

where:

$$\bar{\rho} = \begin{cases} \rho & \text{if} \quad \alpha(0) \in \left(-\frac{\pi}{2}, \frac{\pi}{2}\right] \\ -\rho & \text{otherwise} \end{cases};$$

$$\bar{\alpha} = \begin{cases} \alpha & \text{if} \quad \alpha(0) \in \left(-\frac{\pi}{2}, \frac{\pi}{2}\right] \\ \alpha - \pi & \text{if} \quad \alpha(0) > \frac{\pi}{2} \\ \alpha + \pi & \text{if} \quad \alpha(0) \leq -\frac{\pi}{2} \end{cases};$$

$$\bar{\phi} = \begin{cases} \phi & \text{if} \quad \alpha(0) \in \left(-\frac{\pi}{2}, \frac{\pi}{2}\right] \\ \phi - \pi & \text{if} \quad \alpha(0) > \frac{\pi}{2} \\ \phi + \pi & \text{if} \quad \alpha(0) \leq -\frac{\pi}{2} \end{cases};$$

and the control gains satisfy conditions

$$k_1 > 0, \quad k_3 > 0, \quad k_2 > \frac{4}{\pi}k_1 k_3 \quad . \quad (13)$$

The proposed control law ensures the asymptotic stability of closed-loop visual system. As a first step, consider that if $\alpha(0) \in (-\frac{\pi}{2}, \frac{\pi}{2}]$, then $\alpha(t) \in (-\frac{\pi}{2}, \frac{\pi}{2}]$, $\forall t > 0$, with the above choice of the control gains. In fact, it is sufficient to verify that $\dot{\alpha}$ is always strictly negative for $\alpha = \frac{\pi}{2}$, and it is always strictly positive for $\alpha = -\frac{\pi}{2}$. On the other hand, if $\alpha(0) \in (-\frac{3}{2}\pi, -\frac{\pi}{2}] \cup (\frac{\pi}{2}, \frac{3}{2}\pi)$, by using the state variables $\bar{\alpha}$, $\bar{\phi}$ instead of α, ϕ, and changing the direction of the forward velocity u_1, the same model in eq. (10) is obtained, with the property that $\bar{\alpha}(t) \in (-\frac{\pi}{2}, \frac{\pi}{2}]$, $\forall t > 0$.

Let us consider the following quadratic Lyapunov function candidate: $V = \frac{1}{2}(\rho^2 + \alpha^2 + k_3\,\phi^2)$. Simple computations show that the derivative of V evaluated along the closed loop dynamics (10) with the control input (12) results: $\dot{V} = -k_1|\cos(\alpha)|\rho^2 - k_2\alpha^2 \leq 0$. As in [1], the function V is negative semi-definite. By using the LaSalle invariance principle, the closed-loop system converges to the largest invariant set contained in the set $\Omega = \{(\rho,\ \alpha,\ \phi) : \dot{V} = 0\} = \{(\rho,\ \alpha,\ \phi) : \rho = \alpha = 0\}$. By substituting the control law in system (10), we obtain the closed loop dynamics:

$$\begin{bmatrix} \dot{\rho} \\ \dot{\alpha} \\ \dot{\phi} \end{bmatrix} = \begin{bmatrix} -k_1\cos(\alpha)\rho \\ -k_2\alpha + k_1\frac{\sin(\alpha)}{\alpha}k_3\,\phi \\ k_1\sin(\alpha) \end{bmatrix}. \quad (14)$$

From the second equation it follows that $\dot{\alpha} = k_1 k_3\,\phi$ in every invariant set within Ω. As the system converges to Ω, α and hence $\dot{\alpha}$ tend to zero, then also ϕ tends to zero. As a consequence, the asymptotic stability of

the origin follows from invariant set theorem.

To make a comparison between the control approach in eq. (11), and the modified control system of eq. (12), simulation results are reported in Fig. 2. Three trials are reported corresponding to the initial vehicle configurations $q_1 = [1\ 1.2\ 0]^T$, $q_2 = [1\ 0\ 0]^T$, and $q_3 = [1.2\ -1\ 0]^T$. In all cases, the desired Lagrangian coordinates are $q^{(d)} = (0, 0, 0)$. From observation of fig. 2, it can be easily checked that cusps in the state trajectory may cause features escape quickly from the image plane. As opposite, the closed-loop system with the proposed control law (12) has a regular behavior due to the fact that no inversions of motion occur, since u_1 can not change sign.

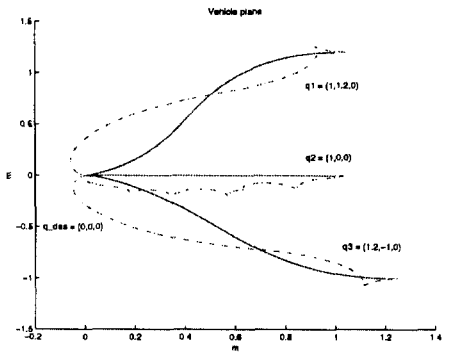

Figure 2: Comparison between the control law proposed in [1] (dotted lines) and the modified version of eq. (12) (continuous lines).

4 Image-Based Dynamic Estimation

To derive the system dynamics in the reduced coordinates of the configuration space, we have implicitly assumed to know the 3-D parameters h_i, $i = 1, \ldots, n$. Unfortunately, for unstructured environments, no a priori knowledge of these 3-D parameters may be available.

In this section, we consider the problem of estimating the unknown, but constant, heights h_i of the environment features, from measurements taken from the vehicle camera. In this phase, we do not use absolute positioning information of the vehicle. However, we do rely on velocity sensors on the vehicle, that are usually available at the wheels (either directly, or by processing of encoder information) of real vehicles.

To verify the identifiability of the 3-D parameters of the environment from visual and velocity information, consider a feature state vector $[X_1, Z_1, h_1, \ldots, X_n, Z_n, h_n]^T$, and its dynamics, expressed in the camera frame $< c >$

$$\begin{cases} \dot{X}_1 = -Z_1\,\omega \\ \dot{Z}_1 = -v + X_1\,\omega \\ \dot{h}_1 = 0 \\ \vdots \\ \dot{X}_n = -Z_n\,\omega \\ \dot{Z}_n = -v + X_n\,\omega \\ \dot{h}_n = 0 \end{cases} \tag{15}$$

Consider the image coordinates, which can be directly measured using the camera, as the output of the above nonlinear system,

$$\begin{cases} x_1 = \frac{f\,X_1}{Z_1} \\ y_1 = \frac{f\,h_1}{Z_1} \\ \vdots \\ x_n = \frac{f\,X_n}{Z_n} \\ y_n = \frac{f\,h_n}{Z_n} \end{cases} . \tag{16}$$

The associated observability codistribution is

$$\partial\mathcal{O} = \begin{bmatrix} \partial\mathcal{O}_1 & 0 & \ldots & 0 \\ 0 & \partial\mathcal{O}_2 & \ldots & 0 \\ \vdots & \vdots & \ddots & \vdots \\ 0 & 0 & \ldots & \partial\mathcal{O}_n \end{bmatrix} . \tag{17}$$

where

$$\partial\mathcal{O}_i = \begin{bmatrix} \frac{f}{Z_i} & -\frac{f\,X_i}{Z_i^2} & 0 \\ 0 & -\frac{f\,h_i}{Z_i^2} & \frac{f}{Z_i^2} \\ \frac{f}{Z_i^2} & -\frac{2\,f\,X_i}{Z_i^2} & 0 \\ -\frac{2\,f\,X_i}{Z_i^2} & \frac{2\,f\,(1+X_i^2)}{Z_i^3} & 0 \\ 0 & -\frac{2\,f\,h_i}{Z_i^3} & \frac{f}{Z_i^2} \\ -\frac{f\,h}{Z_i^2} & \frac{2\,f\,X_i\,h_i}{Z_i^2} & -\frac{f\,X_i}{Z_i^2} \\ \ldots & \ldots & \ldots \end{bmatrix} . \tag{18}$$

By choosing, for each block, the rows 1, 2, and 4, it is easy to verify that $rank(\partial\mathcal{O}) = 3n$. We conclude that there exists inputs to the vehicle that allow to identify 3-D features completely.

Provided that regular persistent inputs [3] are applied to the vehicle, a simple approach to obtain an estimation of parameters h_i, $i = 1, \ldots, n$, which are the only nontrivial unknowns of the problem, consists in rewriting the optical flow equations of the i–th feature (see eq. 2) as

$$\begin{bmatrix} \dot{x}_i \\ \dot{y}_i \end{bmatrix} - \begin{bmatrix} \frac{f^2+x_i^2}{f} \\ \frac{x_i\,y_i}{f} \end{bmatrix} \omega = \begin{bmatrix} -\frac{x_i\,y_i}{f} \\ -\frac{y_i}{f} \end{bmatrix} v\,\bar{h}_i; \tag{19}$$

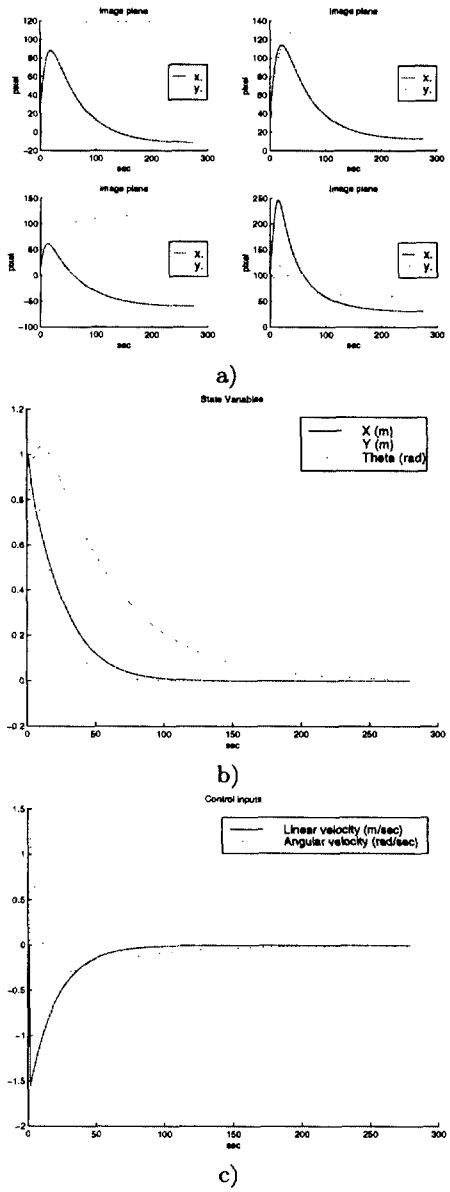

Figure 3: First simulation: control strategy with known height. a) Image coordinates of object points x (pixels); b) Lagrangian coordinates; c) translational and angular velocities v (m/sec), w (rad/sec).

where $\bar{h}_i = \frac{1}{h_i}$. The above expression can be written in matrix form as $A_i = B_i \bar{h}_i, \quad i = 1, \ldots, n$, where $A_i \in \Re^{2\times 1}$ and $B_i \in \Re^{2\times 1}$ are obviously defined. Since the unknown $\bar{h}_i$ appears linearly, a gradient estimator is designed as

$$\dot{\hat{h}}_i = -\frac{p_0}{2}\frac{\partial [e_i^T e_i]}{\partial \hat{h}_i} = -p_0 A_i^T e_i \quad , \qquad (20)$$

where $e_i = \hat{B}_i - B_i = A_i \hat{h}_i - B_i$, and p_0 is a positive gain. The gradient-based estimator can be used in a preliminary self-calibration step in order to recover the 3-D parameters of the target object. The estimates will then be used in the control loop to perform the vehicle-object relative positioning.

5 Simulation Results

Simulation have been performed for different positions of target features. Two trials are reported: the first describes the vehicle behavior when the heights are known and are used in the recovery equations of the centroid; in the second, the off-line 3-D parameters estimation procedure of eq. (20) is applied, and then the estimates are used in the next control phase. The working conditions are the same for both trials: the starting and desired configurations of the vehicle are respectively $\boldsymbol{q}_i = (1, 1.2, \frac{\pi}{4})$, and $\boldsymbol{q}^{(d)} = (0, 0, 0)$; the initial 3-D points coordinates are: $\boldsymbol{P}_1 = (1, -0.1, 1)$, $\boldsymbol{P}_2 = (1, 0.1, 1)$, $\boldsymbol{P}_3 = (2, -1, 2)$ and $\boldsymbol{P}_4 = (3, 1, 2)$; with these values, the initial image points have corresponding coordinates: $\boldsymbol{p}_1 = (25.4, 51.4)$, $\boldsymbol{p}_2 = (34.8, 54.7)$, $\boldsymbol{p}_3 = (18.4, 65.2)$ and $\boldsymbol{p}_4 = (108.5, 80.8)$. The desired values of the image points are : $\boldsymbol{p}_1^{(d)} = (-12, 120)$, $\boldsymbol{p}_2^{(d)} = (12, 120)$, $\boldsymbol{p}_3^{(d)} = (-60, 120)$ and $\boldsymbol{p}_4^{(d)} = (40, 80)$. The sampling time, needed for the image elaboration and control is $50msec$; the gain have been chosen as $k_1 = 1$, $k_2 = 3$, $k_3 = 1$, $p_0 = 0.8$, the focal length of the camera is 120 pixel. The trajectories of image coordinates for the first simulation are shown in Fig. 3. The behaviour of the closed-loop system is satisfactory when the heights of target points are known. Notice that the use of a redundant number of features allows completion of the control task, even with a temporary loss of features visibility. In the second simulation an off-line estimation phase that allows to get approximate values of 3-D parameters is used, results are shown in Fig. 4. True values of heights were $h_1 = 1\,m$, $h_2 = 1\,m$, $h_3 = 2\,m$ and $h_4 = 2\,m$, while the initial estimates $\hat{h}_1 = 2\,m$, $\hat{h}_2 = 0.2\,m$, $\hat{h}_3 = 3\,m$ and $\hat{h}_4 = 1\,m$, (an initial mismatch of up to 100%). From simulation trials, some instructive experience was gained. The control inputs of the self-calibration phase have to be carefully chosen, as high velocities may cause oscillations in the estimates, and visibility of image features must be ensured.

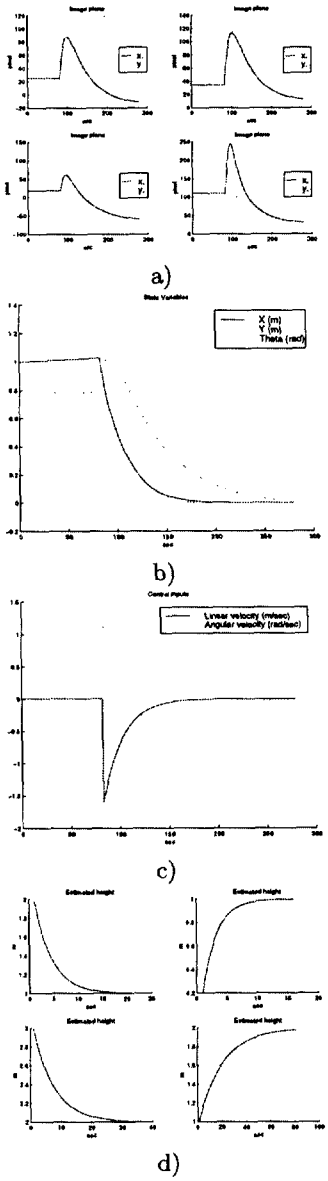

Figure 4: Second simulation: control and height adaptation. a) Image coordinates of object points $\mathbf{x}$ (pixels); b) Lagrangian coordinates; c) translational and angular velocities v (m/s), w (rad/s); d) estimated height h (m).

6 Conclusion

The problem of stabilizing the pose of the mobile robot with respect to a target object of interest using real-time visual data has been investigated. The designed discontinuous feedback control law represents a novel visual servoing technique, which is able to deal with the nonholonomic constraints of the vehicle. Future investigation consists in applying the proposed vision-based technique in robot team coordination tasks, such as self-localization and target following.

References

[1] M. Aicardi, G. Casalino, A. Balestrino, and A. Bicchi. "Closed loop smooth steering of unicycle-like vehicles". In *IEEE Conference on Decision and Control, Lake Buena Vista, FL*, December 1994.

[2] A.M. Bloch, M. Reyhanoglu, and N.H. McClamroch. "Control and stabilization of nonholonomic dynamic systems". *IEEE Trans. on Automatic Control*, 37(11):1746–1757, 1992.

[3] G. Bonard, F. Celle-Couenne, and G. Gilles. *"Observability and observers"*. In Nonlinear Systems, Vol.1, Edited by A.J. Fossard and D. Normand-Cyrot, Chapman & Hall, 1995.

[4] R.W. Brockett. "Asymptotic stability and feedback stabilization". *In Differential Geometric Control Theory, R.S. Millman R.W. Brockett and H.H. Sussmann, (eds)*, 1983.

[5] C. Canudas de Wit and O.J. SØrdalen. "Exponential stabilization of mobile robots with nonholonomic constraints". *IEEE Trans. on Automatic Control*, 37(11):1791–1797, 1992.

[6] R. Frezza, G. Picci, and S. Soatto. "A lagrangian formulation of nonholonomic path following". *In The confluence of vision an control, A. S. Morse et al. (eds), Springer*, 1998.

[7] K. Hashimoto and T. Noritsugu. "Visual servoing of nonholonomic cart". In *IEEE Int. Conf. on Rob. and Autom., Albuquerque, New Mexico*, April 1997.

[8] S. Hutchinson, G.D. Hager, and P.I Corke. "Tutorial on visual servo control". *IEEE Trans. Rob. Autom.*, 12(5):651–670, 1996.

[9] K. Kanatani. *Geometrical Computation for Machine Vision.* Oxford Science Publications, 1993.

[10] A. De Luca, G. Oriolo, and C. Samson. "Feedback control of a nonholonomic car-like robot". *In Robot Motion Planning and Control, J.P. Laumond, (eds), Springer*, 1998.

[11] R.M. Murray and S.S. Sastry. "Nonholonomic motion planning: steering using sinusoids". *IEEE Trans. on Automatic Control*, 38(5):700–716, 1993.

[12] C. Samson. "Control of chained systems. application to path following and time-varying point stabilization". *IEEE Trans. on Automatic Control*, 40:64–77, 1995.

[13] D. Tsakiris, P. Rives, and C. Samson. "Applying visual servoing techniques to control non-holonomic mobile robots". In *IEEE-RSJ International Conference on Intelligent Robots (IROS97), Grenoble, France*, September 1997.